



2

to average 1 hour per response, including the time for reviewing instructions, searching existing data sources, reviewing the collection of information. Send comments regarding this burden estimate or any other aspect of this form to Washington Headquarters Services, Directorate for Information Operations and Reports, 1215 Jefferson Ave., Management and Budget, Paperwork Reduction Project (0704-0188), Washington, DC 20503.

1. AGENCY USE ONLY (Leave blank)		2. REPORT DATE January 24, 1994	3. REPORT TYPE AND DATES COVERED Reprint	
4. TITLE AND SUBTITLE SHARC, A Model for Calculating Atmospheric and Infrared Radiation Under Non-Equilibrium Conditions			5. FUNDING NUMBERS S3411301	
6. AUTHOR(S) R.L. Sundberg*, J.W. Duff*, J.H. Gruninger*, L.S. Bernstein* R.D. Sharma, M.W. Matthew*, S.M. Alder-Golden*, R.J. Healey**, J.H. Brown, D.C. Robertson*				
7. PERFORMING ORGANIZATION NAME(S) AND ADDRESS(ES) Phillips Laboratory/GPOS 29 Randolph Road Hanscom AFB, MA 01731-3010			8. PERFORMING ORGANIZATION REPORT NUMBER PL-TR-94-2010	
9. SPONSORING/MONITORING AGENCY NAME(S) AND ADDRESS(ES)			10. SPONSORING/MONITORING AGENCY REPORT NUMBER	
<p>DTIC SELECTE FEB 1 1994 S C D</p>				
11. SUPPLEMENTARY NOTES *Spectral Sciences Inc., 99 Bedford St., Burlington, MA 01803 **Yap Analytics, Inc., 594 Marrett Rd., Lexington, MA 02173 Reprint from AGU Geophysical Monograph based on the proceedings of the Chapman Conference on the Upper Mesosphere and Lower Thermosphere				
12a. DISTRIBUTION AVAILABILITY STATEMENT Approved for public release; Distribution unlimited			12b. DISTRIBUTION CODE	
13. ABSTRACT (Maximum 200 words) A new computer model, SHARC, has been developed by the Air Force for calculating high-altitude atmospheric IR radiance and transmittance spectra with a resolution of better than 1 cm ⁻¹ . Comprehensive coverage of the 2 to 40 μm (250 to 5,000 cm ⁻¹) wavelength region is provided for arbitrary lines of sight in the 50-300 km altitude regime. SHARC accounts for the deviation from local thermodynamic equilibrium (LTE) in vibrational state populations by explicitly modeling the detailed production, loss, and energy transfer processes among the important molecular vibrational states. The calculated vibrational populations are found to be similar to those obtained from other non-LTE codes. The radiation transport algorithm is based on a single-line equivalent width approximation along with a statistical correction for line overlap. This approach is reasonably accurate for most applications and is roughly two orders of magnitude faster than the traditional LBL methods which explicitly integrate over individual line shapes. In addition to quiescent atmospheric processes, this model calculates the auroral production and excitation of CO ₂ , NO, and NO ⁺ in localized regions of the atmosphere. Illustrative comparisons of SHARC predictions to other models and to data from the CIRRIS, SPIRE and FWI field experiments are presented.				
14. SUBJECT TERMS Non-Local Thermodynamic Equilibrium, Infrared Radiation, Computer Code, Vibrational and Rotational Levels, Limb Radiance			15. NUMBER OF PAGES 16	
			16. PRICE CODE	
17. SECURITY CLASSIFICATION OF REPORT UNCLASSIFIED	18. SECURITY CLASSIFICATION OF THIS PAGE UNCLASSIFIED	19. SECURITY CLASSIFICATION OF ABSTRACT UNCLASSIFIED	20. LIMITATION OF ABSTRACT SAR	

94-03126

200

SHARC,

A Model for Calculating Atmospheric Infrared Radiation Under Non-Equilibrium Conditions

R. L. Sundberg,* J. W. Duff,* J. H. Gruninger,* L. S. Bernstein,*
R. D. Sharma,[§] M. W. Matthew,* S. M. Adler-Golden,* R. J. Healey,[&]
J. H. Brown,[§] and D. C. Robertson*

ABSTRACT

A new computer model, SHARC, has been developed by the Air Force for calculating high-altitude atmospheric IR radiance and transmittance spectra with a resolution of better than 1 cm^{-1} . Comprehensive coverage of the 2 to $40 \mu\text{m}$ (250 to $5,000 \text{ cm}^{-1}$) wavelength region is provided for arbitrary lines of sight in the 50-300 km altitude regime. SHARC accounts for the deviation from local thermodynamic equilibrium (LTE) in vibrational state populations by explicitly modeling the detailed production, loss, and energy transfer processes among the important molecular vibrational states. The calculated vibrational populations are found to be similar to those obtained from other non-LTE codes. The radiation transport algorithm is based on a single-line equivalent width approximation along with a statistical correction for line overlap. This approach is reasonably accurate for most applications and is roughly two orders of magnitude faster than the traditional LBL methods which explicitly integrate over individual line shapes. In addition to quiescent atmospheric processes, this model calculates the auroral production and excitation of CO_2 , NO , and NO^+ in localized regions of the atmosphere. Illustrative comparisons of SHARC predictions to other models and to data from the CIRRIS, SPIRE and FWI field experiments are presented.

1. INTRODUCTION

The calculation of infrared (IR) radiance and transmittance spectra is important in many areas of atmospheric science, including modeling the energy budget, analyzing data from remote sounding experiments, and understanding molecular excitation and production processes. The US Air Force has developed a number of computer codes that can address these applications, including LOWTRAN,¹ MODTRAN,² and FASCODE.³ In the upper altitude regime, more sophisticated models are required to describe deviations from local thermodynamic equilibrium (LTE) as radiative and collisional processes become comparable. An initial non-LTE (NLTE) computer model, HAIRM,⁴ resulted from

[§]Phillips Laboratory, Geophysics Directorate/OS, 29 Randolph Rd., Hanscom AFB, MA 01731-3010

[&]Yap Analytics, Inc., 594 Marrett Rd., Lexington, MA 02173

*Spectral Sciences, Inc., 99 S. Bedford St., Burlington, MA 01803

analyses of the 1977 SPIRE rocket measurements.⁵⁻⁷ In addition, high resolution radiative transport codes, NLTE^{8,9} for the quiescent atmosphere and AARC¹⁰ for auroral conditions, were developed. However, a rapid and unified code spanning a wide range of altitudes and conditions has been lacking.

This paper describes a new NLTE code, SHARC,¹¹ which calculates upper atmospheric IR radiation and transmittance. Its combination of speed and spectral resolution (0.5 cm^{-1}) should make it useful for many applications. The calculational model includes all important IR-active species in the 2-40 μm wavelength region for arbitrary line-of-sight (LOS) paths between 50 and 300 km. It incorporates the bands of NO, CO₂, O₃, H₂O, OH, CO, and CH₄ found in the quiescent atmosphere, including isotopic bands of CO₂, and H₂O. It also accounts for auroral production and excitation of CO₂, NO, and NO⁺ caused by the flux of energetic solar electrons.

In accounting for NLTE effects, molecular vibrational state populations are calculated by explicitly solving the chemical equations for the excitation and relaxation of each vibrational state. As in other NLTE atmospheric models (e.g., Wintersteiner et al.,⁹ Lopez-Puertas et al.^{12,13}), steady-state kinetics are assumed for the quiescent atmospheric processes of collisional excitation, de-excitation, energy transfer, radiative decay, chemical production, and illumination by the sun, earth, and atmosphere. The additional production and excitation mechanisms resulting from electron deposition during auroral storms are included in SHARC using a time-dependent kinetic model.

A profile of vibrational state populations is input to the LOS spectral radiance module, which performs line-by-line (LBL) radiation transport calculations using an equivalent width formalism. This approach uses an algebraic approximation for the total absorption by a single isolated line, resulting in a considerable enhancement in speed compared to the standard LBL grid method, by which we mean explicit integration over individual line shapes. Corrections are made for line overlap. As will be discussed below, typical radiance differences with this approach are less than 10%.

SHARC is available for use by the scientific community and may be obtained from the Air Force Phillips Laboratory/GPOS, 29 Randolph Rd., Hanscom AFB, MA 01731.

2. CODE DESCRIPTION

The schematic in Fig. 1 illustrates SHARC's module structure and overall calculational sequence. The input module is a menu-driven user interface. Atmospheric temperature and species density profiles are specified via an external file. Profiles are

ion For
CRA&I
TAB
collected
heat m

ation /

Availability Code	
Dist	Avail and/or Special
A-1	

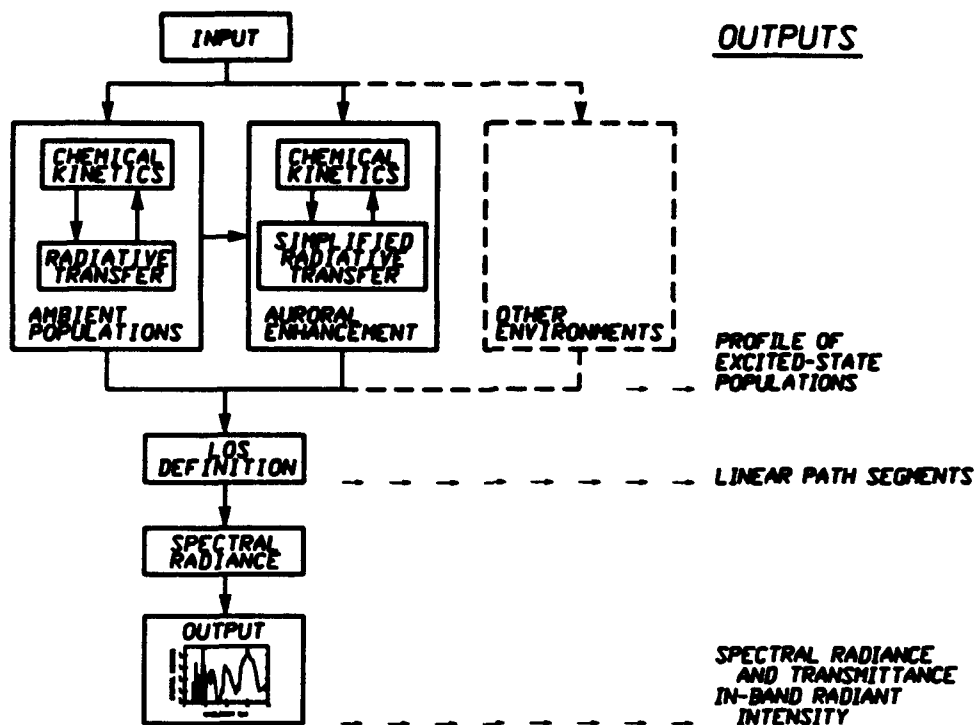


Figure 1. SHARC Module Structure and Calculational Sequence.

required for the IR-active species (NO, CO₂, H₂O, O₃, CO, OH, and CH₄), the major atmospheric species to which they are collisionally coupled (N₂, O₂, O), and atomic hydrogen, whose reaction with O₃ provides the main source of OH(v). Other input parameters include LOS specifications and, if desired, the coordinates of a localized auroral region through which the LOS may pass.

Altitude profiles of excited vibrational state populations are calculated in the chemical kinetics and radiative transfer modules and saved in a data file for later use. Under auroral conditions, a time-dependent chemical model then calculates the additional production of CO₂, NO, and NO⁺ arising from interactions of auroral electrons. To generate the desired LOS spectrum, the vibrational state populations are fed to the spectral radiance module, which outputs radiance and transmittance spectra and in-band intensities.

Condensed descriptions of the calculations are given below. Additional information may be found in the SHARC Users Manual.¹¹ Code upgrades in progress or planned are indicated by the dotted lines in Fig. 1. These include: a generalized generator for atmospheric profiles of IR-active species based on scaling of MSIS¹⁴ profiles; extending the spectral region into the near IR and visible regions; and provisions for multiple, distinct atmospheric regions, for use in modeling the solar terminator, tidal and gravity waves, or other atmospheric inhomogeneities.

2.1 Quiescent Chemical Kinetics

The quiescent chemical kinetics are handled primarily through separate reaction sets for each IR-active molecule; these sets are solved individually in each layer of the atmosphere to obtain the excited vibrational state population profiles. Atmospheric layers are assumed to be horizontally uniform and typically 2 to 10 km in height. The reaction database files contain the list of vibrational states for each molecule and the equations for the chemical reactions and rate constants written in symbolic form. These equations include chemical formation of excited vibrational states, collisional deactivation and excitation (satisfying detailed balance), spontaneous emission, and the radiative excitation processes associated with absorption of radiation from the sun and from the atmosphere. The size of the database is indicated in Table 1.

Table 1. Quiescent Radiating Species in SHARC.

<u>Molecule</u>	<u>Isotopes</u>	<u>States</u>	<u>Reactions</u>	<u>Bands</u>
CO ₂	3	84	664	113
H ₂ O	4	32	128	36
O ₃	1	30	176	45
NO	1	3	5	3
CO	1	3	9	3
OH	1	10	32	24
CH ₄	1	12	52	13

The SHARC CHEMKIN module, which is based on the Sandia CHEMKIN general-purpose chemical kinetics code,¹⁵ reads the reaction files and sets up the time-dependent differential rate equations. The quiescent vibrational state number density [M*] in each atmospheric layer is obtained from the solution to the steady-state equations. The species CO₂(v), H₂O(v), and OH(v) are indirectly coupled to each other via resonant energy transfer processes involving N₂(v=1).^{16,17} The steady-state equations for these species are linearized by equating the ground vibrational state number densities to the total number densities and then solving for the N₂(v=1) population.

The collisional rate constants were obtained from the recent literature and from Taylor's review¹⁸ of measurements prior to 1974; details are given elsewhere.¹⁹ The solar excitation rates are derived using the LOS radiation transport model discussed below. For

solar zenith angles greater than 90°, MODTRAN² is used to account for the attenuation of sunlight by the atmosphere below 50 km. The earthshine excitation rates are expressed in terms of an effective blackbody temperature corresponding to the altitude where the vibrational band becomes optically thick in a nadir view.

The calculation of the radiative excitation rate, r_a , of molecular vibrational states due to emission originating from atmospheric layers in the 50-300 km altitude range is performed in a subroutine dubbed NEMESIS and follows the treatment of Kumer and co-workers.^{16,17} For a given vibrational band, the population enhancements of the vibrational states are expressed via a set of linear equations,

$$[M^*_i] - [M^*_i]_0 = \alpha_i \omega_i \sum_j P_{ji} \omega_j [M^*_j] \quad , \quad (1)$$

where α_i is the probability for absorption of a photon entering layer i , P_{ji} is the probability that a photon emitted from layer j will be absorbed in layer i , and ω_j is the branching ratio for re-emission. Both the P matrix elements and the α_i depend on the populations of the lower vibrational states. Therefore, the calculation proceeds in stages to solve for successively higher-energy states. The first CHEMKIN run (with all $r_a = 0$) defines the ground state populations $[M_i]$ and the initial excited state populations $[M^*_i]_0$ for transitions to the ground state. The results are used in NEMESIS to evaluate (P) and α_i and to compute the radiative excitation rates r_a for those transitions. CHEMKIN is then rerun including the r_a to generate the corresponding populations for the next set of vibrational transitions. The CHEMKIN/NEMESIS sequence is repeated until solutions for the highest energy states are obtained.

The major calculational effort in NEMESIS is computing the P matrix elements, which involves a multidimensional integral over the location, direction, vibration-rotation line, frequency location within the line, and propagation distance of the emitted photons within each layer. The integral is evaluated with the aid of Monte Carlo sampling using trial "photons". The calculation assumes semi-infinite plane-parallel geometry and uses the Voigt line shape.

The CHEMKIN/NEMESIS calculations were verified by comparing vibrational temperatures for NLTE vibrational states of CO₂, which are both solar and earthshine pumped, with calculations by other workers. These profiles of vibrational temperatures are consistent with the results of Wintersteiner et al.⁹ and Lopez-Puertas et al.,²⁰ who used different computer algorithms but similar chemical kinetic models and atmospheric profiles. Typical results from SHARC are shown in Fig. 2. The vibrational states are

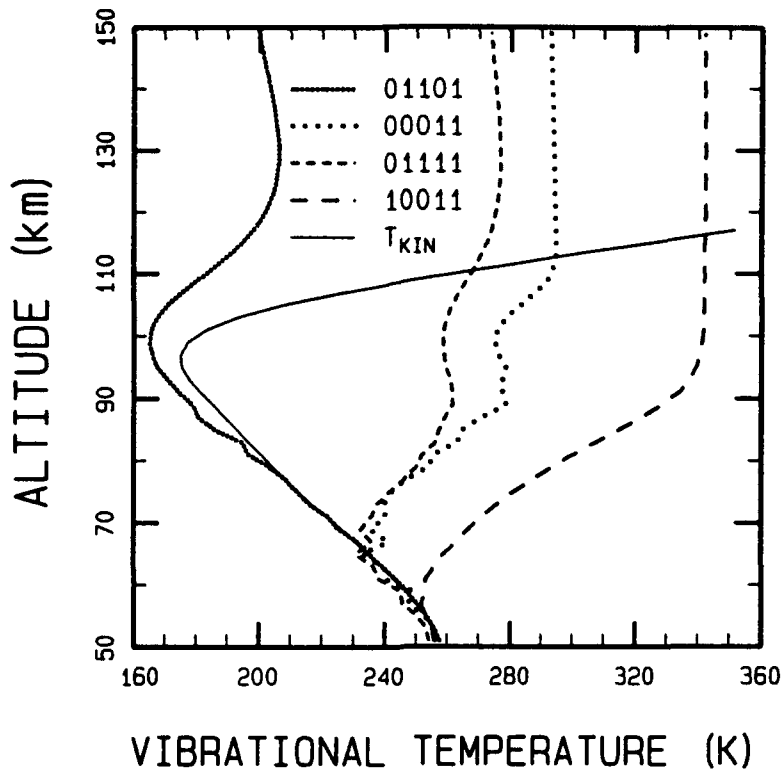


Figure 2. Calculated Vibrational Temperatures for CO₂ States for a Solar Zenith Angle of 82°.

labeled using the HITRAN²¹ convention. The fine structures in the profiles are numerical noise from the Monte Carlo calculations.

2.2 Auroral Kinetics and Radiation Transport

The auroral kinetics model calculates the enhancements of CO₂, NO, and NO⁺ radiation resulting from energy deposited in the upper atmosphere by solar electrons. Approximately 600 time- and energy-dependent rate equations are used to calculate the secondary electron distribution (in fourteen energy bins) and the subsequent reactive and energy-transfer processes. The energy deposition model for the primary electrons is based on work by Grün, Rees, and Strickland²²⁻²⁴ as implemented in the Air Force Phillips Laboratory code AARC.¹⁰ The chemical reactions and energy transfer processes used in SHARC are described in Refs. 19 and 25.

The integration of the time-dependent differential equations is accomplished using the Gear algorithm supplied with the Sandia CHEMKIN code.¹⁵ The use of time-dependent kinetics results in an improvement over the steady-state treatment used, for

example, in AARC.¹⁰ According to SHARC, the NO($v=1$) production efficiency per ion pair increases with time during the aurora. This results from collisional excitation of the increasing concentration of ground state NO, whereas in AARC the efficiency remains constant.

The emissions from NO and NO⁺ are both optically thin and prompt; by prompt, we mean that the excited states radiatively decay before they have a chance to relax collisionally. Therefore, coupling of the radiative transfer and collisional processes is not required, and the solutions to the excitation mechanisms for each layer suffice. However, CO₂ ν_3 emission below 100 km is both optically thick and delayed, so that coupling the CO₂ time-dependent chemical kinetics to a radiative transfer scheme is required. With the present kinetic scheme, a full treatment would require either solving approximately 4000 coupled differential equations or repeating the radiative excitation calculations (CHEMKIN/NEMESIS) at each time increment. Since these are impractical, a modified escape function approximation,²⁵ which assumes that photons emitted from a given layer either escape the atmosphere or are re-absorbed within the layer, has been adopted. To insure the correct limit for negligible auroral excitation, SHARC includes a correction which forces a match to the exact NEMESIS solution for ambient conditions. This correction consists of a time-independent source or sink term added to the differential equation for excitation of CO₂ ν_3 .

2.3 Line-of-Sight Spectral Radiance Model

In order to determine the LOS spectral radiance, the LOS properties are represented in terms of a sequence of homogeneous segments. The spectral radiance contribution of a single emission line, j , to a single segment, i , is modeled by

$$I_{ij}(\nu) = \frac{1}{\Delta\nu} R_{ij} \left[\xi_i W_{ij} - \xi_{i-1} W_{(i-1)j} \right] , \quad (2)$$

where ν is the central frequency of the calculational spectral interval of width, $\Delta\nu$, R_{ij} is the emission source function, W_{ij} is the cumulative equivalent width for the LOS path from the observer through the i 'th segment, and ξ is a correction factor which accounts for line overlap. The total path spectral radiance is determined by direct summation of I_{ij} over all segments and lines.

The emission source term is derived directly from the kinetically determined excited-state vibration rotation populations and is given by

$$R_{ij} = \frac{C_1 \nu^3}{\pi} \frac{\gamma_{ij}}{1 - \gamma_{ij}} \quad (3)$$

where C_1 is the first radiation constant and γ_{ij} is the ratio of the upper-to-lower state vibration-rotation populations. This expression for R_{ij} reduces to the Planck blackbody function in the limit in which all the vibration-rotation state populations are specified by the local gas temperature, i.e., LTE conditions.

In the limit of no line overlap ($\xi=1$) Eq. (2) is exact provided that the equivalent widths are exactly determined, such as by explicit frequency integration over the line shape function. However, this is computationally time consuming. By using the approximations described below, a rapid evaluation can be achieved with only a modest sacrifice of accuracy (about $\pm 10\%$).

The equivalent widths W_{ij} for single lines are calculated using the Rodgers-Williams²⁶ approximations for Voigt line shapes,

$$W_{ij}^2 = W_v^2 = \alpha_D \frac{2}{\ln 2} \left[W_L^2 + W_D^2 - \left(\frac{W_L W_D}{W_W} \right)^2 \right] \quad (4)$$

where the subscripts V, D, L, and W refer to the Voigt, Doppler, Lorentz, and weak-line limits, and $\alpha_D(\text{cm}^{-1})$ is the Doppler linewidth. W_D , W_L , and W_W are calculated from the approximations given by Ludwig et al.,²⁷ which are accurate to within 8% or better, using Curtis-Godson^{28,29} path-averaged line parameters. The line strengths and air-broadened half-widths are tabulated in a file generated from the HITRAN atlas²¹ that has been supplemented with lines for NO^+ and higher vibrational states of NO and O_3 .

The line overlap correction is based on the statistical overlap approximation in which it is assumed that there is no positional correlation among the lines in the calculational spectral interval. This approximation accounts for line wing overlap within the spectral interval but does not include the contribution of line wings from lines centered outside the interval. The correction factor is given by

$$\xi_i = \Delta\nu \left[1 - \prod_j \left(1 - \frac{W_{ij}}{\Delta\nu} \right) \right] / \sum_j W_{ij} \quad (5)$$

In applying this spectral radiance model, it is implicitly assumed that the calculational spectral interval width, $\Delta\nu$, is larger than the largest single-line equivalent width for the entire LOS. This limits the calculational spectral resolution to about 0.5 cm^{-1} for tangent paths near the lower atmosphere boundary of 50 km. However, higher spectral resolution can be used for non-limb paths or limb paths with higher-altitude tangent points.

The accuracy of this LOS radiance algorithm has been explored through comparisons to standard high-resolution LBL grid calculations for typical atmospheric conditions. A number of different regimes were investigated, including vertical and horizontal viewing geometries, optically thin and thick lines, multiple overlapping lines and bands, and LTE and NLTE conditions. Figures 3a and 3b show SHARC limb radiance calculations for just CO₂ in the ν_2 spectral region at tangent altitudes of 50 and 75 km, respectively. Each figure also includes the absolute value of the difference spectrum which was obtained by subtracting a LBL grid method calculation from the SHARC calculations. A major source of error in the SHARC calculations is the statistical line overlap approximation. This approximation under-corrects for line overlap when the emission lines in a given spectral interval are nearly degenerate. This can be seen in the 50 km limb calculation shown in Figure 3a for the Q branch near 597 cm⁻¹ and leads to a 20% over prediction for the radiance over a 2 cm⁻¹ spectral interval. The line overlap approximation over-corrects for line overlap when the emission lines in a spectral interval are nearly equally spaced. This occurs in the calculation shown in Figure 3a in the Q branch near 667 cm⁻¹ and leads to an error of 10%. For LOS's and bands which have less line overlap, such as the 75 km limb calculation in Figure 3b, peak errors remain below 10%. The SHARC calculation is roughly two orders of magnitude faster than a LBL calculation using FASCODE.

3. DATA COMPARISONS

While comparisons with other computer codes can verify the numerical algorithms, upper atmospheric IR data are needed to assess the reasonableness of the various model assumptions, including kinetic mechanisms, rate constants, and properties of the atmosphere. To illustrate typical levels of agreement between field data and model calculations in diverse applications, several comparisons of SHARC predictions and data from US Air Force-sponsored field experiments are presented.

The CIRRI-1A experiment³⁰ conducted on the Space Shuttle STS-39 during April, 1991, collected the first extensive set of limb IR radiance spectra over a wide altitude range using a sensitive cryogenic Michelson interferometer with a spectral resolution of 1 cm⁻¹. A typical quiescent nighttime spectrum in the 780-1250 cm⁻¹ spectral region is shown in Figs. 4a and 4b; the tangent height at the center of the detector FOV is about 64 km. For clarity in plotting, the resolution of the original spectrum has been degraded to 3 cm⁻¹ FWHM. The major features are CO₂ hot bands near 791 cm⁻¹ and 961 cm⁻¹, the ν_3

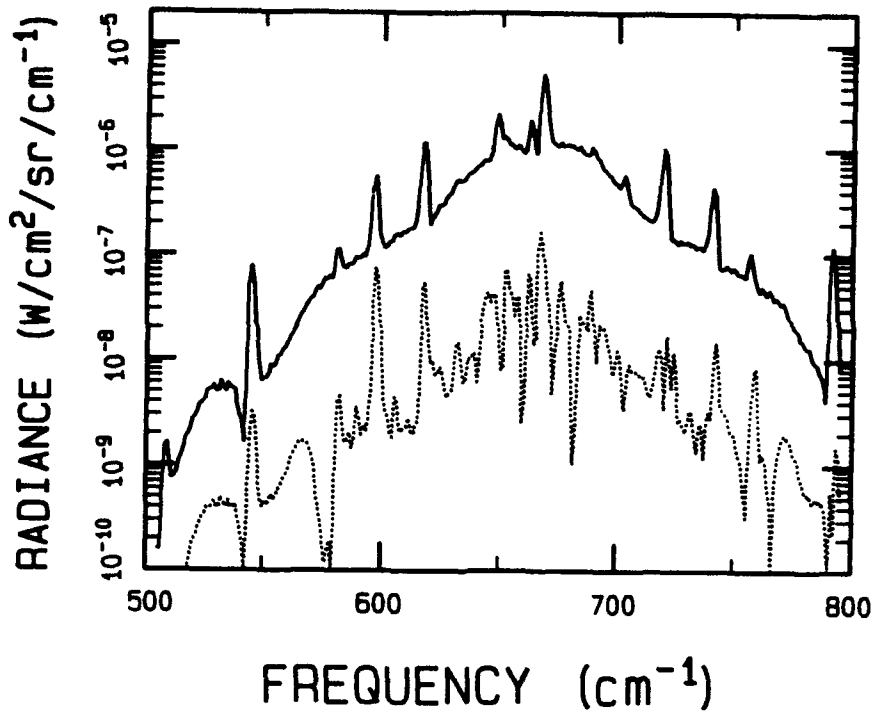


Figure 3a. SHARC (Solid) and SHARC minus LBL Difference (Dotted) Spectra for CO₂ Radiance for a 50 km Limb View.

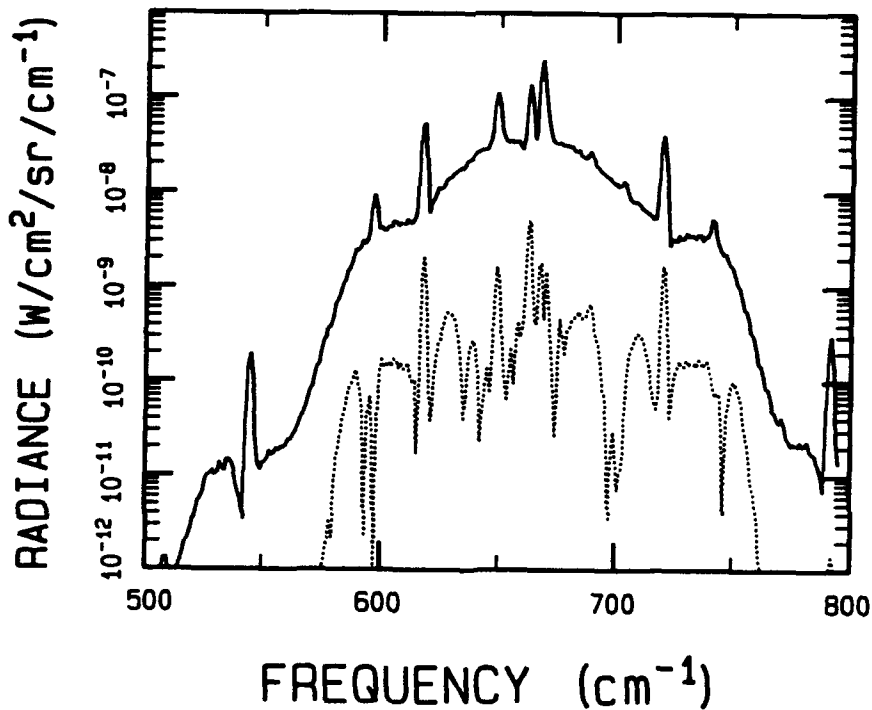


Figure 3b. SHARC (Solid) and SHARC minus LBL Difference (Dotted) Spectra for CO₂ Radiance for a 75 km Limb View.

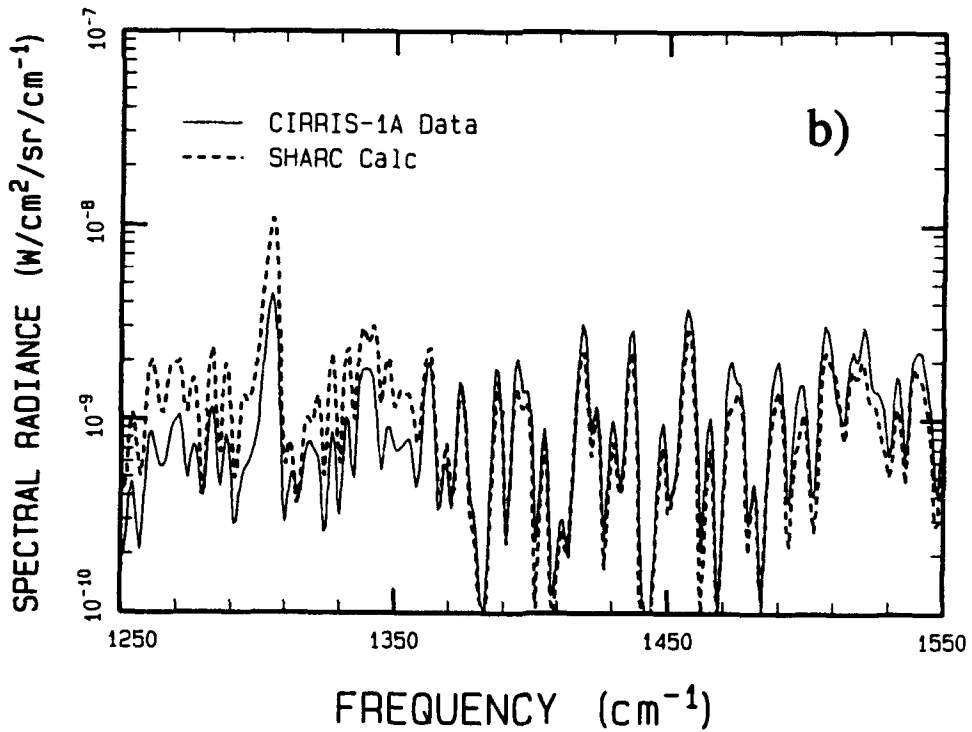
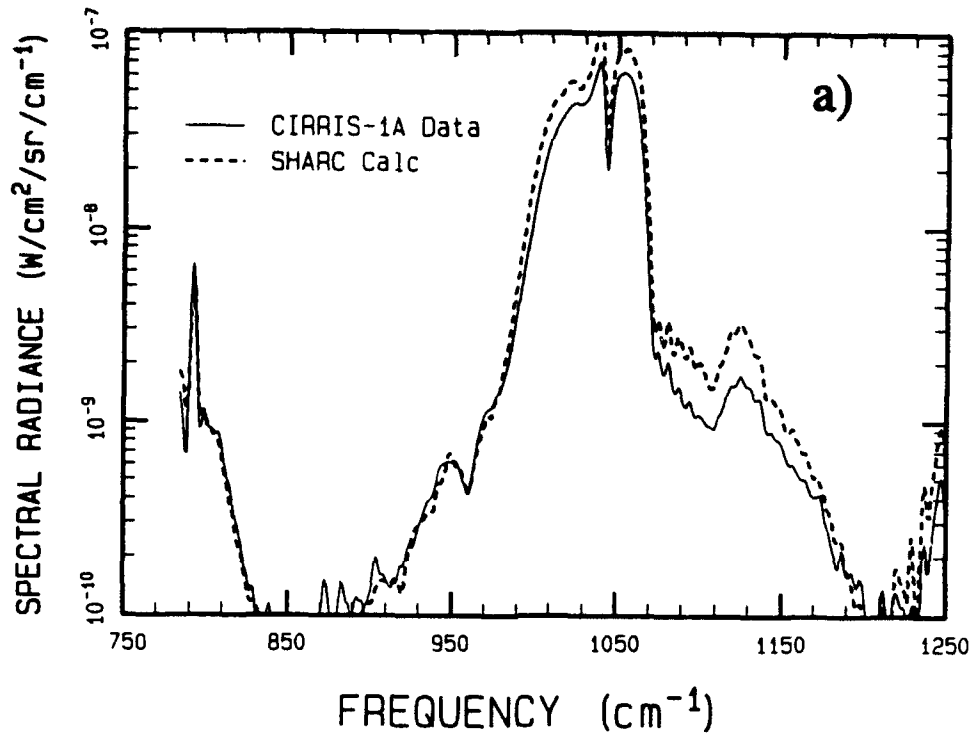


Figure 4. Quiescent Nighttime Limb Spectrum from the CIRRIS-1A Experiment³⁰ Near 64 km Tangent Height and SHARC Simulation.

(1042 cm^{-1}) and ν_1 (1103 cm^{-1}) bands of O_3 , the ν_4 band of CH_4 near 1311 cm^{-1} , and resolved lines of the ν_2 band of H_2O , which dominate the spectrum beyond around 1370 cm^{-1} . The overlaid SHARC calculation, performed for similar viewing conditions, reproduces the observed spectral structure throughout this region. The up to factor-of-two differences in the absolute intensities of some bands are ascribed to differences in species concentrations between the actual atmosphere and the model atmosphere, which is derived from the NRL Trace Gas Climatology database.³¹

Data for upper atmospheric CO_2 ν_3 emission and its dependence on solar angle is provided in Fig. 5, which shows the limb radiance measured in an earlier rocket experiment, SPIRE,³² launched from Poker Flat Research Range, Alaska near the dawn terminator. Different phenomena dominate the excitation depending on the altitude regimes. During the day, the primary isotope is solar-excited above 110 km, while at lower altitudes the radiance is enhanced by pumping of the 2.7 μm band and by emissions

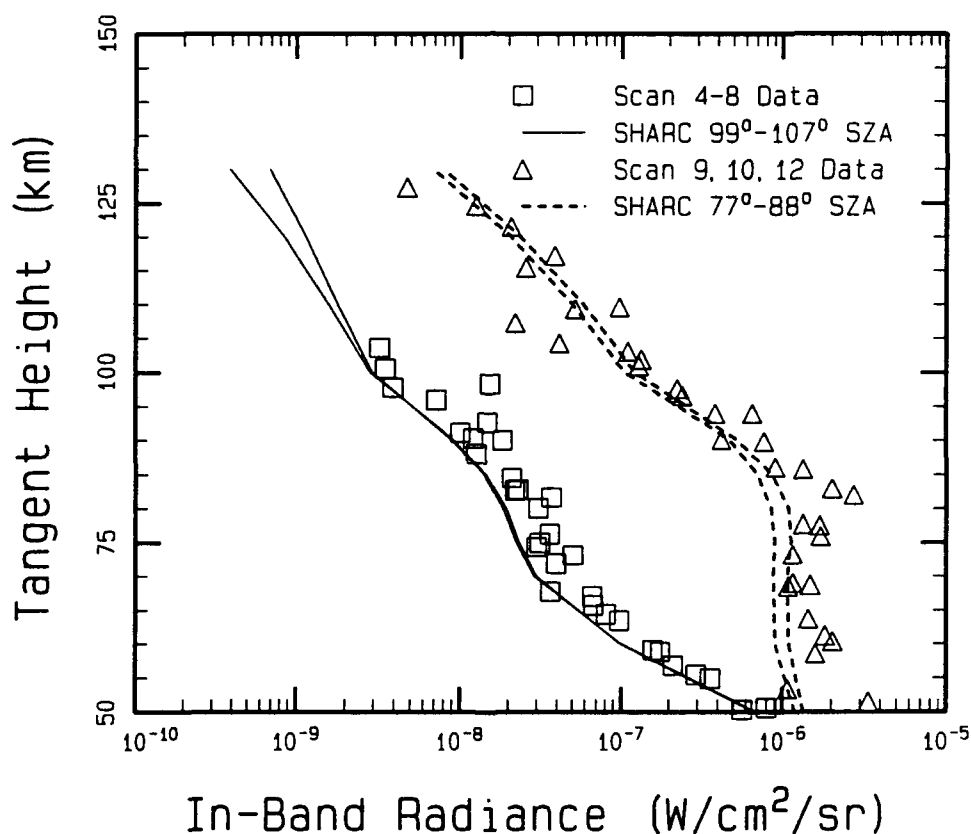


Figure 5. CO_2 4.3 μm Band Limb Radiance Measured in the SPIRE Rocket Experiment³² and Predicted by SHARC for Different Solar Zenith Angles Near the Dawn Terminator.

from hot bands and minor isotopes.^{6,33} As the density increases, the widening line shape makes the single-quantum excitation of the primary isotope again important with contributions from multiple quantum bands at 1.6, 2.0, and 2.7 μm .⁶ The SPIRE data and the SHARC calculations agree to within the data scatter, which averages around a factor of two.

An example of SHARC's capability to calculate auroral radiance enhancements is shown in Fig. 6. A nitric oxide spectrum from the Field-Widened Interferometer rocket experiment,³⁴ which observed an IBC Class II aurora, is compared with a SHARC model calculation at a resolution of 1 cm^{-1} . The auroral calculation uses energy deposition parameters described by Picard et al.³⁵ The reaction of metastable nitrogen atom, $\text{N}(^2\text{D})$, with molecular oxygen has been assumed to be the only source of NO chemiluminescence in the SHARC auroral model. The overall band shape, which includes strong aurorally induced hot band contributions, is reproduced well by the calculation, except near the edges of the band where NLTE rotational populations, not currently modeled, yield enhanced high rotational lines. The calculated absolute radiance is a factor of four lower

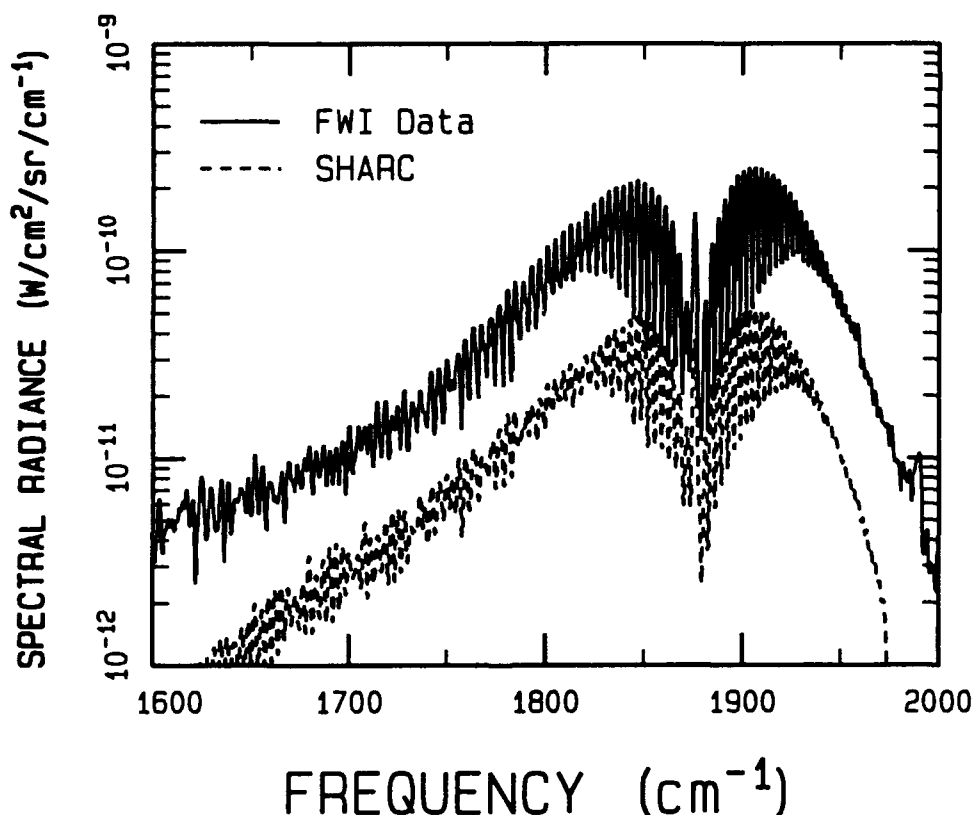


Figure 6. Calculated and Observed³⁴ NO Spectrum for Zenith Viewing Through a Class II Aurora from 90 km Altitude.

than the data. Solomon³⁶ and Gérard et al.³⁷ have suggested that the reaction of translationally hot $N(^4S)$ with O_2 may be an important contributor to NO formed in the thermosphere. Sharma et al.³⁸ have presented calculations that show that the reaction of $N(^4S)$ atoms with O_2 accounts for recent observations of highly rotationally excited NO vibrational emissions in the dayglow.³⁹ Finally, the reactions of $N(^4S)$ and $N(^2D)$ with O_2 may lead to a quantitative explanation of NO formed in recent artificial auroral experiments.⁴⁰ Given the uncertainties associated with characterization of the aurora and as well as the role of $N(^4S)$ in the formation of NO, the agreement between the model and data is encouraging.

Numerous other data and model comparisons have been and are currently being performed for all the major atmospheric IR emission bands during daytime, nighttime, and auroral conditions. The results will be reported in future papers.

4. CONCLUSION

A new computer model, SHARC, has been developed by the Air Force for rapid LBL calculation of NLTE upper atmospheric IR radiance and transmittance spectra with a resolution of 1.0 cm^{-1} or better. SHARC treats the important molecular vibrational bands from 2 to $40 \mu\text{m}$ (250 to $5,000 \text{ cm}^{-1}$) for arbitrary lines of sight in the 50-300 km altitude range, accounting for the detailed production, loss, and energy transfer processes among the important vibrational states. Calculated vibrational temperatures agree with results from other NLTE codes,^{9,10,13} and the equivalent-width spectral algorithm used in LOS radiation transport calculations results in a considerable time savings over grid LBL methods that explicitly integrate over the full line shape.

Comparisons of SHARC radiance predictions with field measurements, especially those from CIRRI 1A, are ongoing. Comparisons performed to date indicate reasonable agreement for most emission bands, including the CO_2 $4.3 \mu\text{m}$ feature, which poses a good test for different aspects of the code. Planned upgrades include a solar terminator module and extension of the spectral region down to the near IR. Data simulations using SHARC have applications to remote sensing of the upper atmosphere, such as deriving density profiles for species like NO, O_3 , and H_2O , which have significant atmospheric variability.

5. ACKNOWLEDGEMENTS

The authors wish to thank Dr. A.J. Ratkowski and Dr. W.A.M. Blumberg (Phillips Laboratory/GPOS) for their support during the development of SHARC and Mr. R.M.

Nadile of the Phillips Laboratory/GPOS for providing the emission spectrum from the CIRRIS 1A measurements. The authors also wish to acknowledge Dr. V.I. Lang of the Aerospace Corp. for reviewing the chemical kinetic database. This work was funded by the Ballistic Missile Defense Organization (formerly SDIO) under PMA 1105.

6. REFERENCES

1. F.X. Kneizys, G.P. Anderson, E.P. Shettle, W.O. Gallery, L.W. Abreu, J.E.A. Selby, J.H. Chetwynd, and S.A. Clough, "Users Guide to LOWTRAN 7," AFGL-TR-88-0177, (NTIS No. ADA 206773) (1988).
2. G.P. Anderson, J.H. Chetwynd, J.-M. Theriault, P. Acharya, A. Berk, D.C. Robertson, F.X. Kneizys, M.L. Hoke, L.W. Abreu, and E.P. Shettle, "MODTRAN2: Suitability for Remote Sensing," *SPIE Proc.*, 1968 (1993)
3. S.A. Clough, F.X. Kneizys, E.P. Shettle, and G.P. Anderson, "Atmospheric Radiance and Transmittance: FASCOD2", *Proc. of the Sixth Conference on Atmospheric Radiation*, pp. 141-144, Am. Met. Soc., Boston, MA (1986).
4. T.C. Degges and A.P. D'Agati, "A User's Guide to the AFGL/Visidyne High Altitude Infrared Radiance Model," AFGL-TR-85-0015 (NTIS No. ADA 161432) (1985).
5. A.T. Stair, Jr., R.D. Sharma, R.M. Nadile, D.J. Baker, and W.F. Grieder, "Observations of Limb Radiance with Cryogenic Spectral Infrared Rocket Experiment," *J. Geophys. Res.*, **90**, 9763 (1985).
6. R.D. Sharma and P.P. Wintersteiner, "CO₂ Component of Daytime Earth Limb Emission at 2.7 μm ," *J. Geophys. Res.*, **90**, 9789 (1985)
7. R.D. Sharma and R.J. Healey, "Earthlimb Emission Analysis of Spectral Infrared Rocket Experiment (SPIRE) Data at 2.7 μm - A 10 Year Update," *SPIE Proc.*, 1540 (1991)
8. R.D. Sharma, R.D. Siani, M.K. Bullitt, and P.P. Wintersteiner, "A Computer Code to Calculate Emission and Transmission of Infrared Radiation Through Non-Equilibrium Atmospheres," AFGL-TR-83-0168 (NTIS No. ADA 137162) (1983).
9. P.P. Wintersteiner, R.H. Picard, R.D. Sharma, J.R. Winick, and R.A. Joseph, "Line-by-Line Radiative Excitation Model for the Non-Equilibrium Atmosphere: Application to CO₂ 15- μm Emission," *J. Geophys. Res.*, **97**, 18083 (1992).
10. J.R. Winick, R.H. Picard, R.D. Sharma, R.A. Joseph, and P.P. Wintersteiner "Radiative Transfer Effects on Aurora Enhanced 4.3 Micron Emission," *Adv. Space Res.*, **7**, 17-21 (1987).
11. R.D. Sharma, J.W. Duff, R.L. Sundberg, L.S. Bernstein, J.H. Gruninger, D.C. Robertson, and R.J. Healey, "Description of SHARC-2, The Strategic High-Altitude Radiance Code," PL-TR-91-2071, (NTIS No., ADA 239008) (1991).

12. M. Lopez-Puertas, R. Rodrigo, A. Molina, and F.W. Taylor, "A Non-LTE Radiative Transfer Model for Infrared Bands in the Middle Atmosphere, I, Theoretical Basis and Application to CO₂ 15 μm Bands," *J. Atmos. Terr. Phys.*, **48**, 729 (1986).
13. M. Lopez-Puertas, R. Rodrigo, J.J. Lopez-Moreno, and F.W. Taylor, "A Non-LTE Radiative Transfer Model for Infrared Bands in the Middle Atmosphere, II, CO₂ (2.7 and 4.3 μm) and Water Vapor (6.3 μm) Bands and N₂(1) and O₂(1) Vibrational Levels," *J. Atmos. Terr. Phys.*, **48**, 749 (1986).
14. A.E. Hedin, "Extension of the MSIS Thermospheric Model into the Middle and Lower Atmosphere," *J. Geophys. Res.*, **96**, 1159 (1991).
15. R.J. Kee, J.A. Miller, and T.H. Jefferson, "CHEMKIN: Problem-Independent, Transportable, Fortran Chemical Kinetics Code Package," Sandia Rpt. No. SAND80-8003, Sandia National Laboratory, Livermore, CA 94550 (1980).
16. J.B. Kumer and T.C. James, "CO₂ (001) and N₂ Vibrational Temperatures in the 50 ≤ Z ≤ 130 km Altitude Range," *J. Geophys. Res.*, **79**, 638 (1974).
17. J.B. Kumer, "Atmospheric CO₂ and N₂ Vibrational Temperatures at 40- to 140-km Altitude," *J. Geophys. Res.*, **82**, 16 (1977).
18. R.L. Taylor, "Energy Transfer Processes in the Stratosphere," *Can. J. Chem.*, **52**, 1436 (1974).
19. D.C. Robertson, P.K. Acharya, S.M. Adler-Golden, L.S. Bernstein, F. Bien, J.W. Duff, J.H. Gruninger, R.L. Sundberg, R.J. Healey, J.M. Sindoni, P.M. Bakshi, A. Dalgarno, and B. Zygelman, "Investigations into Atmospheric Radiative Processes in the 50-300 km Regime," PL-TR-91-2137, (NTIS No. ADA 251588) (1991).
20. M. Lopez-Puertas, M.A. Lopez-Valverde, C.P. Rinsland, and M.R. Gunson, "Analysis of the Upper Atmosphere CO₂(ν₂) Vibrational Temperatures Retrieved From ATMOS/Spacelab 3 Observations," *J. Geophys. Res.*, **97**, 20469 (1992).
21. L.S. Rothman, R.R. Gamache, A. Goldman, L.R. Brown, R.A. Toth, H.M. Pickett, R.L. Poynter, J.M. Flaud, C. Camy-Peyret, A. Barbe, N. Husson, C.P. Rinsland, and M.A.H. Smith, "The HITRAN Molecular Database: Editions of 1991 and 1992," *J. Quant. Spectrosc. Radiat. Transfer*, **48**, 469 (1992).
22. A.E. Grün, "Luminescenz-photometrische Messungen der Energieabsorption im Strahlungsfeld von Elektronenquellen Eindimensionaler Fall im Luft," *Z. Naturforsch.*, **112a**, 89-95 (1957).
23. M.H. Rees, "Auroral Ionization and Excitation by Incident Energetic Electrons," *Planet. Space Sci.*, **111**, 1209-18 (1964).
24. D.J. Strickland, J.R. Jasperse, and J.A. Whalen, "Dependence of Auroral FUV Emissions on the Incident Electron Spectrum and Neutral Atmosphere," *J. Geophys. Res.*, **88**, 8051-62 (1983).
25. J.B. Kumer, "Theory of the CO₂ 4.3 μm Aurora and Related Phenomena," *J. Geophys. Res.*, **82**, 2203 (1977).

26. C.D. Rodgers and A.P. Williams, "Integrated Absorption of a Spectral Line with the Voigt Profile," *J. Quant. Spectrosc. Radiat. Transfer*, **14**, 319 (1974).
27. C.B. Ludwig, W. Malkmus, J.E. Reardon, and J.A. Thomson, *Handbook of Infrared Radiation From Combustion Gases*, SP-3080, Scientific and Technical Information Office, NASA, Washington DC (1973).
28. A.R. Curtis, "A Statistical Model for Water Vapour Absorption," *Q. J. R. Meteorol. Soc.*, **78**, 638-640 (1952)
29. W.L. Godson, "The Evaluation of Infrared-Radiative Fluxes due to Atmospheric Water Vapour," *Q. J. R. Meteorol. Soc.*, **79**, 367-379 (1953).
30. D.R. Smith, W.A.M. Blumberg, R.M. Nadile, S.J. Lipson, E.R. Huppi, and N.B. Wheeler, "Observation of High-N Hydroxyl Pure Rotation Lines in Atmospheric Emission Spectra by the CIRRIS-1A Space Shuttle Experiment," *Geophys. Res. Lett.*, **19**, 593 (1992).
31. M.E. Summers, W.J. Sawchuck, and G.P. Anderson, "Model Climatologies of Trace Species in the Atmosphere," Annual Review Conference on Atmospheric Transmission Models, Phillips Laboratory, Hanscom AFB, MA 01731 (June 1992)
32. A.T. Stair, Jr., R.D. Sharma, R.M. Nadile, D.J. Baker, and W.F. Grieder, "Observations of Limb Radiance with Cryogenic Spectral Infrared Rocket Experiment," *J. Geophys. Res.*, **90**, 9763 (1985).
33. J.B. Kumer, R.M. Nadile, and W. Grieder, "Detailed Analysis of 4.3 μm Earthlimb Data," *SPIE Proceedings*, **430**, 244, SPIE, Box 10, Bellingham, WA 98227 (1983)
34. P.J. Espy, C.R. Harris, A.J. Steed, J.C. Ulwick, R.H. Haycock, and R.A. Straka, "Rocketborne Interferometer Measurement of Infrared Auroral Spectra," *Planet. Space Sci.*, **36**, 543 (1988).
35. Picard, R.H., J.R. Winick, R.D. Sharma, A.S. Zachor, P.J. Espy, and C.R. Harris, "Interpretation of infrared measurements of the high-latitude thermosphere from a rocketborne interferometer," *Adv. Space Res.*, **7**, 23-30 (1987).
36. Solomon, S., "The possible effects of translationally excited nitrogen atoms on lower thermospheric odd nitrogen," *Planet. Space Sci.*, **31**, 135-139 (1983).
37. Gérard, J.-C., V.I. Shematovich, D.V. Bisikalo, "Non thermal nitrogen atoms in the Earth's thermosphere 2. a source of nitric oxide," *Geophys. Res. Lett.*, **18**, 1695-1698 (1991).
38. Sharma, R.D., Y. Sun, and A. Dalgarno, "Highly rotationally excited nitric oxide in the terrestrial thermosphere," *Geophys. Res. Lett.*, **20**, 2043-2045 (1993).
39. Armstrong, P.S., S.J. Lipson, J.R. Lowell, W.A.M. Blumberg, D.R. Smith, R.M. Nadile, and J.A. Dodd, "Analysis of comprehensive CIRRIS 1A observations of nitric oxide in the thermosphere," *Eos Trans AGU*, **74**, 225 (1993).
40. Lipson, S.J., P.S. Armstrong, J.R. Lowell, W.A.M. Blumberg, D.E. Paulsen, M.J. Fraser, W.T. Rawlins, D.B. Green, R.E. Murphy, and J.A. Dodd, "Mission-wide EXCEDE III nitric oxide spectroscopic analysis," *Eos Trans AGU*, **74**, 225 (1993).